



Elaboration of nanostructured polyurethane foams/OMMT using a twin-screw extruder in the counter-rotating mode

YASMINE MAHMOUD^{1*}, ZITOUNI SAFIDINE¹ and HICHEM ZEGHIOUD²

¹Laboratoire de Chimie Macromoléculaire, Ecole militaire Polytechnique, BP 17, Bordj El Bahri, Algeria and ²Laboratoire de Génie des Procédés, Université Badji Mokhtar, Annaba, Algeria

(Received 21 March, revised 14 September, accepted 18 September 2018)

Abstract: In this work, a new elaboration method for nanostructured foam polyurethane/organo-modified montmorillonite (PUR/OMMT) by *in situ* polymerization is proposed. A twin-screw extruder in the contra-rotation mode combined with reaction injection molding (RIM) as the polymerization process was used. The blended polyols, copolymer polyol (CPP) were included between the OMMT layers via the twin-screw extruder. Both the formulation of the PUR and the inter-foliar distance in the montmorillonite (MMT) were optimized. The effect of some parameters such as OMMT content and catalyst (triethylenediamine for PUR 3 and triethylenediamine+diamino-1,2 propane for PUR 4) was also investigated. The synthesized materials (OMMT, PUR and PUR/OMMT) were characterized by different methods, *i.e.*, Fourier transform infrared spectroscopy (FTIR), X-ray diffraction (XRD) and scanning electron microscopy (SEM). The results of evaluation tests, such as flammability and the tensile for the PUR 3+OMMT foams revealed that the optimum properties were obtained for PUR 3+2 % OMMT. The PUR 4 foam showed better mechanical and flame-retardant properties than the PUR 3 ($r = -\text{NCO}/-\text{OH} = 1.15$) foam. However, the PUR 4 + 2 % OMMT formula exhibited the most delayed flame diffusion and pronounced rigidity.

Keywords: nanocomposite; PUR rigid foam; OMMT; flame retardant.

INTRODUCTION

In the last years, polymer materials have gained ground in replacing so-called conventional materials, such as wood, metals and ceramics. These materials have a wide range of applications because of many advantages, in particular lightweight, durability, corrosion inertia, ease of implementation and low cost. Among these materials, alveolar polymers in general and alveolar polyurethane in particular are distinguish. This latter one is widely used in protection and decoration, the auto-

* Corresponding author E-mail mahmoudyasmine9@gmail.com
<https://doi.org/10.2298/JSC180321076M>

motive, naval, furniture and building industries, and for shock absorption, padding and thermal or acoustic insulation.^{1–5} PUR foams are present in all areas of daily life due to their various properties and applications. Despite all these advantages, these foams can constitute a peril in the event of fire. Currently, public opinion is very aware of this inflammability problem. Among the solutions to address this issue is the addition of organic flame-retardants in the polymer matrix.^{6–8} However, most organic flame-retardants emit toxic gases.

Nevertheless, both researchers and industrialists are interested in finding other solutions, such as the addition of graphite,^{9–12} fibers,^{13,14} montmorillonite,^{15–26} nanocoating,^{27,28} etc. The addition of montmorillonite in the polyurethane imparts noteworthy improvement to the relevant properties, especially if it is distributed on the nanometric scale. It enhances mechanical, thermal, barrier and flame retardant properties.³ These improvements depend on the type of polymer, the ingredients used, the preparation process and the dispersion of the clay in the matrix.^{3,29,30}

Much work on the development of polyurethane foams modified with montmorillonite are reported in the literature.^{15,21–23,31–33} However, the use of a combination of grafted polyol (CPP) and polymeric diphenylmethane diisocyanate (PMDI) and/or diamino-1,2 propane as a catalyst has not been considered.

The main goal of the present study consisted in the preparation of nanostructured foam polyurethane/OMMT with enhanced mechanical and flame-retardant properties. In order to incorporate the grafted polyols into the OMMT galleries, a twin-screw extruder operated in the counter-rotating mode was used. In this study, two formulations of PUR were optimized and used for the preparation of nanocomposite rigid foams. For the first formulation 2, 3, 5, 7 and 10 wt. % of OMMT were used and for the second formulation only 2 wt. % of the OMMT was used. The spectral, morphological and mechanical proprieties of the synthesized material were investigated.

EXPERIMENTAL

Materials

Polyether polyols grafted with 10 % styrene acrylonitrile (SAN) chains, called copolymer polyol (CPP) or polymer polyether polyol (POPE) were supplied by Confortchem. Polymeric methane diphenyl diisocyanate (PMDI) with 30 % NCO was supplied by BASF, triethylenediamine (A-33) used as a catalyst was purchased from Struktol, glycerol ($C_3H_{10}O_3$) was obtained from PanReac, silicone L-580 from Niax, dichloromethane (CH_2Cl_2 , 99.8 %) was supplied by AcroSeal. Diamino-1,2-propane ($C_3H_{10}N_2$, >98 %), sodium chloride (NaCl, 99 %), ammonium acetate (NH_4OAc , $C_2H_7NO_2$, ≥98 %), potassium chloride (KCl, 99 %), ethanol (CH_3CH_2OH , ≥99.8 %), Methylene blue ($C_{16}H_{18}ClN_3S$) and methyl red ($C_{15}H_{15}N_3O_2$) were purchased from Sigma-Aldrich. Hydrochloric acid (HCl, 35–37 %) was purchased from Biochem. Hydrogen dioxide (H_2O_2 , 10 v/v) was obtained from Saidal and the intercalating agent, octadecylamine (ODA, 90 %) was obtained from Fluka. Foundry bentonite (BNT), mined from the Hammam-Boughrara layer of Maghnia, was kindly supplied by Bentel.

Bentonite treatments

The purification of the BNT consisted in the elimination of the all impurities, such as quartz and calcite, and then MMT was extracted by application of various physicochemical treatments.

In order to extract MMT and remove the quartz particles present in the BNT, a suspension of BNT in water (10 wt. %) was allowed to settle during 70 h, and then the aqueous solution was centrifuged in order to recover the MMT. The recovered MMT was treated with 0.1 M HCl (10 g of MMT immersed in 250 mL of 0.1M HCl) at room temperature for 4 h, followed by H₂O₂ (10 %) treatment, *i.e.*, 10 g of MMT dispersed in 500 mL of H₂O₂ for 24 h followed by heating at 70 °C for 30 min.

In order to obtain a uniform MMT surface, a cation exchange was necessary. Thus, 10 g of purified MMT were dispersed in 500 mL NaCl solution (0.5 M) at 70 °C for 4 h. The operation was repeated three times to reach the saturation of the MMT with sodium cations, giving sodium montmorillonite MMT–Na⁺.

The cation exchange capacity (*CEC*) of the MMT–Na⁺ was determined by saturating this MMT–Na⁺ with NH₄⁺ using 1 M ammonium acetate (NH₄OAc) at pH 7. The excess salt was removed by washing with an ethanol–water mixture. Then, the NH₄⁺ ions were displaced by K⁺ using 100 mL of 1 M KCl, solution at pH 2.5.³⁴

The NH₄⁺ concentration was determined according to Norm NF T 90-015-1. Thus, 10 mL of aqueous phase recovered at the end of the NH₄⁺ replacement by K⁺ ions was distilled into a flask containing 10 mL of a 30 % solution of NaOH in 2 % boric acid in the presence of Tashiro's indicator (methylene blue (0.1 %) and methyl red (0.03 %)). The distillation was continued with water until the receiving vessel contained 50 mL. This distillate was titrated with 0.1 M HCl until the indicator color changed from green to light grey.

The *CEC* of the sample was obtained from the following equation:

$$\text{CEC / mmol g}^{-1} = \frac{V_{\text{HCl}} C_{\text{HCl}}}{10g_{\text{MMT-Na}^+}} 10^4 \quad (1)$$

where, *CEC* is the cation exchange capacity of the sample expressed in mmol g⁻¹ of MMT–Na⁺, *C_{HCl}* is the concentration of hydrochloric acid in mole L⁻¹ and *V_{HCl}* is the volume of hydrochloric acid in L⁻¹. The *CEC* value was 1 mmol g⁻¹.

Finally, alkylammonium ions (ODA) were used to modify the hydrophilic nature of the MMT–Na⁺. Grafting of ODA into MMT was realized using an ODA/MMT ratio (mmol/g) equal to two time a *CEC* value as follows: 10⁻² mol of ODA were introduced in 1 L of 0.01 M HCl at 80 °C under mechanical stirring. After three hours, 5 g of MMT–Na⁺ was added. After 20 h of cation exchange, the obtained OMMT was filtered and washed with distilled water at 80 °C. In order to eliminate the physisorbed alkylammonium ions, the MMT was washed after removal of the chloride ions with a previously heated water/ethanol mixture (\approx 70 °C). When the suspension had been completely filtered, dried at 85 °C, crushed and sifted, it was stored in a desiccator.

Formulation of polyurethane foam

The final structure of the polyurethane foams (resulting in the polycondensation reaction of polyol with isocyanate) depends on the reagent used and on the ratio –NCO/–OH:

$$r = \frac{-\text{NCO}}{-\text{OH}} = \frac{\text{Number of functions, kg}}{\text{Number of functions OH, kg}} \quad (2)$$

In the present case, Eq. (2) becomes:

$$r = \frac{-\text{NCO}}{-\text{OH}} = \frac{\text{Number of functions} - \text{NCO from PMDI}}{\text{Number of functions} - \text{OH} + \text{Number of functions} - \text{OH from glycerol}} \quad (3)$$

The calculated amounts of polyol (CPP), glycerol, silicone oil and the catalyst (A-33) were mixed and stirred with an ultra-turrax (30 s). Then the calculated amounts of PMDI and dichloromethane were added and the mixture stirred for 4 to 5 s at a predetermined speed of 6000 rpm and the mixture was injected into the mussel system of the RIM process.

In order to optimize the formulation, several ratios were tested (r of 1.05, 1.10, 1.15, 1.20, 1.25 and 1.30). Only the formulation with $r = 1.15$ was retained and denoted PUR 3. With this same ratio, other plates were prepared but with a combination of two catalysts, *i.e.*, A-33 and diamino-1,2 propane. The stirring time was 12 s and the formula called PUR 4. The agitation time, cream time and rise time for both formulas are summarized in Table I.

TABLE I. Formula of polyurethane the retained foams

Parameter	PUR 3	PUR 4
Content of CPP, %	42.75	42.25
Content of glycerol, %	7.84	7.75
Content of A-33, %	3.92	4.07
Content of diamino-1,2 propane, %	—	0.97
Content of silicone, %	2.36	2.33
Content of PMDI, %	39.21	38.76
Content of CH_2Cl_2 , %	3.92	3.87
Agitation time, s	4	12
Cream time, s	25	25
Rise time, s	35	35

Preparation of nanocomposites

In order to prepare the nanocomposite PUR/OMMT foams, the three components OMMT, CPP and silicone were mixed for 20 min using the ultra turrax instrument at 6000 rpm. Then the mixture was introduced into a twin-screw extruder used in the counter-rotating mode at 80 °C, for 20 min. The CPP molecules were incorporated into the clay layers by adding the other reactants, as was the case with the PUR 3 and 4 foams. It should be noted that this technique is the association of two methods, melt polymerization and *in situ* polymerization. For the PUR 3 formula, 2, 3, 5, 7 or 10 wt. % OMMT was added and for the PUR 4 formula, only 2 wt. % of OMMT was added.

Characterization

The Fourier transform infrared (FTIR) spectra were recorded between 400 and 4000 cm^{-1} from KBr pellets on a Shimadzu type 8400 S infrared Fourier transform spectrometer. The X-ray powder diffraction patterns were recorded on a PANalytical X'Pert PRO diffractometer fitted with CuK_{α} radiation ($\lambda = 1.5404 \text{ nm}$) at 40 kV and 40 mA in the 4–60° 2θ region. The surface morphologies of the samples were investigated *via* scanning electron microscopy (SEM, FEI pattern Quanta 600 at 15 kV), in order to observe the evolution of the structure of the cell and their sizes after incorporation OMMT. For the preparation of the SEM samples, the sample was cut and coated with a thin gold layer, using a Cressington 108 auto sputter coater sputter, with a current intensity of 40 mA, for 30 s. The tensile testing of the rigid poly-

urethane foams was performed on an LLOYD instrument TM, with a load cell of 20 kN. The crosshead speed was set to 5 mm min⁻¹. Samples were cut to polyhedron dimensions 127 mm×10 mm×9 mm, the size between the detectors is 50 mm. The bulk density of the samples foams was estimated by directly measuring the weight and volume of the polyhedron foams.

The test of the flammability of the polyurethane foam sample was evaluated according to the standard UL 94, used by American laboratories. This evaluation was realized according to the UL 94 HB (horizontal burning) and to UL 94V (vertical burning). This test was used for the prepared polyurethane foam samples that had the dimensions 127 mm×12.7 mm×12.7 mm. Marks were indicated on the sample at 25.4 mm (1") and 101.6 mm (3").

RESULTS AND DISCUSSION

Characterization of montmorillonite

Fourier transform infrared spectroscopy (FTIR). The FTIR spectra of foundry BNT, MMT, MMT–Na⁺ and OMMT samples are shown in Fig. 1.

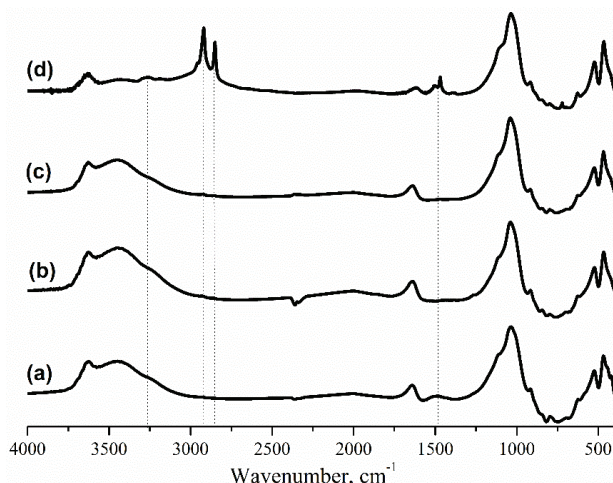


Fig. 1. FTIR spectra of: a) foundry BNT, b) MMT, c) MMT–Na⁺ and d) OMMT.

The disappearance of the peak at 1492 cm⁻¹ attributed to the bending of the C–H group³⁵ from the BNT spectrum (Fig 1a) after purification (MMT spectrum), indicates the elimination of organic compounds presented in the BNT. This result shows that the purification was successfully accomplished. After organophilic modification, new peaks at 3263 and 1466 cm⁻¹ appeared, which could be attributed to the stretching and bending vibrations of the C–N group, respectively.^{35,36} In the OMMT spectrum, the characteristic peaks at 2918 and 2853 cm⁻¹ were associated to C–H stretching,^{22,37,38} showing the existence of organic functions. The strong absorption band at 1040 cm⁻¹ could be assigned to the bending modes of Si–O–Si groups.^{38,39}

X-Ray diffraction pattern (XRD). The X-ray diffraction patterns of the foundry BNT, MMT–Na⁺ and OMMT are presented in Fig. 2.

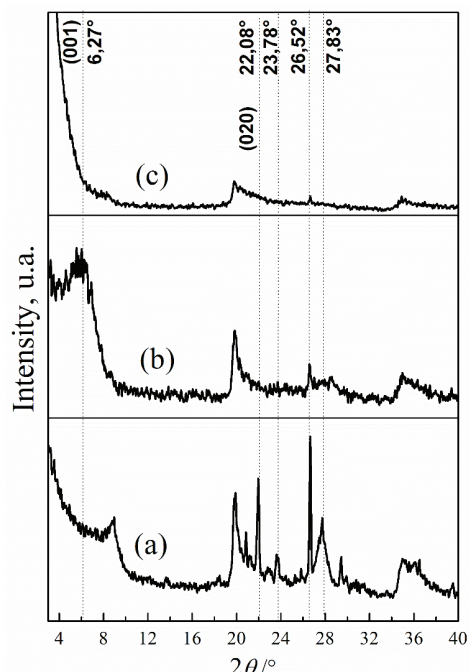


Fig. 2. X-Ray diffraction patterns of: a) foundry BNT, b) MMT- Na^+ and c) OMMT.

The X-ray diffraction pattern of the foundry BNT, MMT- Na^+ and OMMT presented in Fig. 2 confirm the extraction and purification of MMT by the absence of peaks specific to quartz at $2\theta = 22.1, 23.8, 26.5$ and 27.8° in the pattern of MMT- Na^+ ,⁴⁰ and the increase in the basal spacing $d(001)$ after the organophilic modification. This basal spacing was 29.3 Å for the OMMT sample, whereas this distance was only 10 Å for the untreated foundry BNT.

The $d(001)$ was calculated from the position of the (001) reflection using the Braggs equation:

$$n\lambda = 2ds\sin\theta \quad (4)$$

where n is the order of the reflection, in general 1, λ is the wavelength of the X-rays, d is the distance between two layers of the crystals and θ is the angle of the incident X rays.

The foundry BNT showed the characteristic peak at $2\theta = 8.91^\circ$, corresponding to a $d(001)$ spacing of 9.91 Å. For MMT- Na^+ , the peak of montmorillonite was found at $2\theta = 6.27^\circ$, corresponding to a $d(001)$ spacing of 14.06 Å. This increase in the $d(001)$ spacing of MMT- Na^+ also reported by Kherroub *et al.*,⁴¹ could be attributed to the aggressive ion exchange of the calcium cations (100 pm) by sodium cations (102 pm). Similar results were found in the work of El Acha-by *et al.*,³⁸ who reported change in MMT- Na^+ by 2-(1-hydroxyethyl)-1,3-dihexadecyl-benzimidazolium bromide (Bz), where the distance increased from 14.06 Å to 29 Å.

Characterization of polyurethane foams and polyurethane/OMMT nanocomposite foams

Fourier transform infrared spectroscopy (FTIR). The FTIR spectra of PUR 3 and PUR 4 foams, shown in Fig. 3, reveled the appearance of characteristic peaks at 1530 cm^{-1} and at 3437 cm^{-1} , which were attributed to the free N–H absorption and the stretching vibrations of the N–H urethane groups, respectively.^{9,41} Narrows bands at 2977 and 2871 cm^{-1} , both corresponding to the deformation of CH₂ bond, and other C–H bond vibrational modes at 1458 , 1410 and at 1226 cm^{-1} , were also observed.⁴²

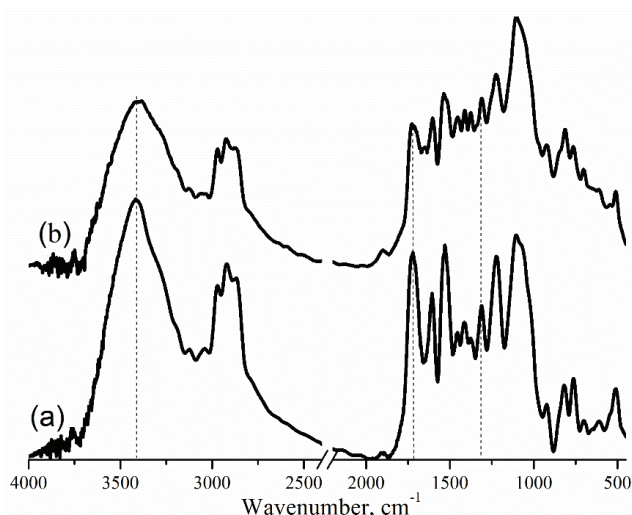


Fig. 3. FTIR spectra of: a) PUR 3 and b) PUR 4.

The band at 1654 cm^{-1} corresponds to the CO stretching vibration of the free urethane and ester groups of the polyol. The band at approximately 1721 cm^{-1} , was assigned to free and hydrogen bonded urethanes (the hydrogen bond between the carbonyl and hydrogen atoms (from OCONH groups)). Furthermore, the band at 1396 cm^{-1} is related to the asymmetric stretching vibrations of the OCONH links.^{3,42} The peak at 1315 cm^{-1} is related to the C–N stretching vibration of the urethane group.^{43,44} Relative increase in the intensity of the characteristic peaks of C–N and the free CO function of PUR 4 were also observed.

The FTIR spectra for PUR 3, PUR 3/OMMT, PUR 4 and PUR 4/OMMT foams are shown in Figs. 4 and 5. The reinforcement of the PUR 3 and PUR 4 by OMMT did not affect the location and the shape of the obtained bands. The increase in the intensity of the bands located between 780 and 1060 cm^{-1} is attributed to the vibrations of groups specific to OMMT, together with vibrations of the groups specific to PUR 3 and PUR 4.

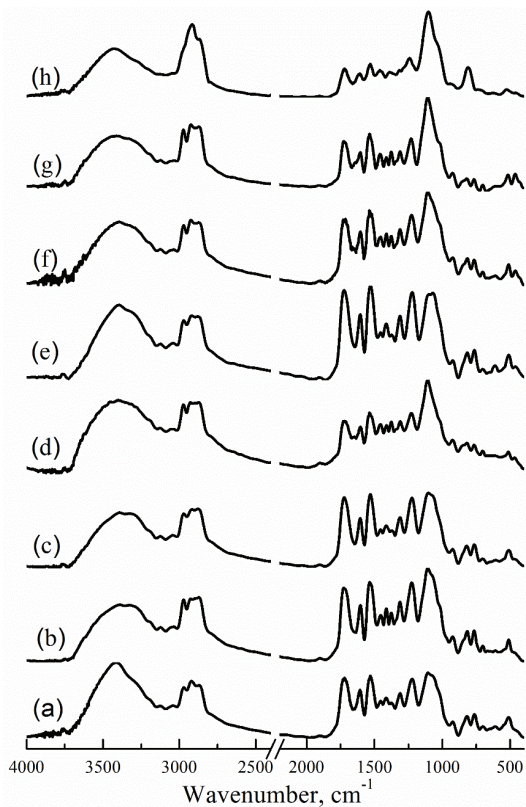


Fig. 4. FTIR spectra of: a) PUR 3, b) PUR 3 + 2 % OMMT, c) PUR 3 + 3 % OMMT, d) PUR 3 + 5 % OMMT, e) PUR 3 + 7 % OMMT, f) PUR 3 + 10 % OMMT, g) PUR 3 + 15 % OMMT and h) PUR 3 + 20 % OMMT.

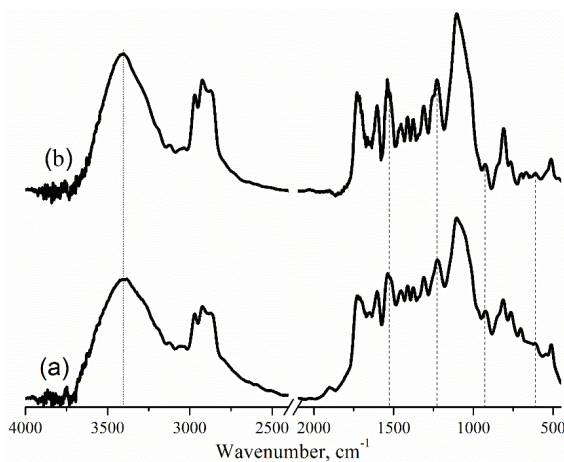


Fig. 5. FTIR spectra of: a) PUR 4 and b) PUR4 + 2 % OMMT.

The broadening of the band at 3420 cm⁻¹ (stretching vibration of N–H groups) observed for OMMT amounts in the PUR foam greater than 5 % could be explained by the presence of hydrogen bonds, which hinder molecular movement.

Flammability tests UL 94V-0, UL 94V-1 and UL 94V-2. The UL 94 vertical test was performed as shown in Fig. S-2 of the Supplementary material to this paper and the results are given in Table II.

TABLE II. Results of the UL 94V-0, UL 94V-1 and UL 94V-2 flammability tests; none of the samples formed incandescent drops on the cotton

Sample	Average combustion time, s	UL 94 verticals classifications		
		V-0	V-1	V-2
PUR 3	127	Yes	Yes	Yes
PUR 3 + 2% OMMT	130	Yes	Yes	Yes
PUR 3 + 3% OMMT	120	Yes	Yes	Yes
PUR 3 + 5% OMMT	110	Yes	Yes	Yes
PUR 3 + 7% OMMT	120	Yes	Yes	Yes
PUR 3 + 10% OMMT	118	Yes	Yes	Yes
PUR 4	154	No	No	No
PUR 4 + 2% OMMT	135	Yes	Yes	Yes

In the both the UL 94 HB (Table S-I of the Supplementary material) and UL 94 V flammability tests, a protective carbon layer, called “char”, was formed in the debris of the test pieces of the rigid polyurethane foams. This proves the possibility of reducing the burning time by the addition of flame-retardants. The results obtained during the application of the flammability test UL 94 confirmed that when OMMT was added to the PUR 3 formula, the combustion time increased. The optimum time was obtained when the OMMT level was 2 %. This could be attributed to a better dispersion of the OMMT in the polymer matrix. Indeed, in light of the obtained results, the burning time of PUR 4 decreased on addition of 2 % OMMT for both the UL94 HB and UL 94 V tests. However, on the other hand, it was classified according to UL 94 V. The burning time of PUR 4 was greater than that of PUR 3, which could be explained by the presence of the diamino-1,2 propane catalyst.

Tensile properties. In order to estimate the tensile properties of rigid foam polyurethanes, five patterns were tested. The apparatus records the stress according to the strain. At the end of the test, the device also recorded the Young's modulus, tensile strength and the elongation at break. The results obtained in this test for the various studied samples of PUR foams are listed in Table III and the stress-strain curves for composites are shown in Fig. S-3 of the Supplementary material.

It can readily be seen from Table III that there is a proportional relationship between the added clay content and the apparent density of the prepared materials. This density decreases sharply when OMMT was added and then increases with increasing OMMT content. This decrease in density is due to the pattern cells formed by the foam, *i.e.*, it was noticed that the foam with 2 % of OMMT

was formed of open cells that contain other cells (presented in the SEM micrographs section).

TABLE III. Results of the tensile test

Formula	Apparent density, kg dm ⁻³	Young's modulus, MPa	Tensile strength at break, MPa	Elongation at break, %
PUR 3	0.4000±0.0091	226.6±23.1	0.525±0.005	3.03±0.10
PUR 3 + 2% OMMT	0.1700±0.0031	674.1±3.3	0.531±0.020	1.15±0.12
PUR 3 + 3% OMMT	0.2070±0.0054	122.1±91.1	0.210±0.018	1.03±0.09
PUR 3 + 5% OMMT	0.2610±0.0092	162.4±6.4	0.188±0.007	4.96±0.17
PUR 3 + 7% OMMT	0.2170±0.0045	148.0±5.2	0.385±0.010	1.63±0.12
PUR 3 + 10% OMMT	0.2550±0.0041	379.8±3.3	0.625±0.015	1.95±0.07
PUR 4	0.5340±0.0033	458.9±1.2	2.546±0.007	4.63±0.18
PUR 4 + 2% OMMT	0.2080±0.0021	345.4±5.1	0.730±0.013	4.09±0.20

Moreover, we have an increase in the Young's modulus increased by 197 and 67 %, for the composites PUR 3 charged with 2 and 10 % OMMT compared to PUR 3, respectively. This increase was probably due to closed cells for the PUR 3 + 10 % OMMT composite. Nevertheless, the Young's modulus of the PUR 3 + 2 % OMMT composite increased despite having open cells. A similar result was found by Saha *et al.*⁴⁵ The other composites PUR 3 foam displayed a decrease in the Young's modulus. This could be due to the perturbation of the polyurethane foams structure in the presence of clay nanoparticles, which disrupt hydrogen bonds.

It is important to report that the Young's modulus for PUR 4 was double that of PUR 3. This could be explained by the strengthening due to hydrogen bond interactions, which increase in the presence of the diamino-1,2 propane. The mechanical proprieties of PUR 4 were decreased when 2 % of OMMT was added, *i.e.*, the density and the Young's modulus decreased by 61 and 24 %, respectively. These decreases are probably due to perturbation of the hydrogen bond formed between the PUR, diamino-1,2 propane and OMMT. However, PUR 4 formula presents optimal mechanical properties, compared to the other samples.

X-Ray diffraction patterns (XRD). The X-ray diffraction patterns of the samples PUR 3 and PUR 3/OMMT in different amounts are presented in Fig. 6. The polyurethane foams prepared by Moawed,⁴⁶ Yang *et al.*,⁴⁷ Lian *et al.*⁴⁸ and Liu *et al.*⁴⁹ had the same shape and peak characteristic as those elaborated in this work.

The X-ray diffraction for all PUR 3 foam samples, both loaded and unloaded showed a large peak centered at $2\theta = 20^\circ$, which were not influenced by the addition of montmorillonite. This peak shows the amorphous character of the polyurethane foam, which was not influenced by the addition of the OMMT in one hand but may, on the other hand, indicate that the layers of OMMT are exfoliated or intercalated. Similar results were reported by Zheng *et al.*⁸ This

peak at $2\theta = 20^\circ$, characterizing the PUR chains is at the reflection plane (110) corresponds to a d -spacing between the chains of 0.442 nm.⁵⁰

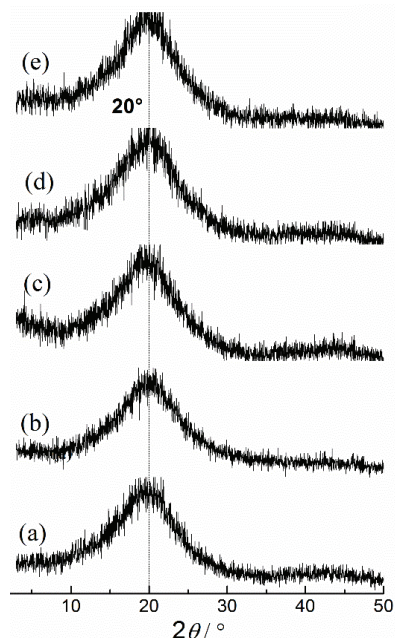


Fig. 6. Juxtaposition of the X-ray diffractograms of the PUR 3 + OMMT nanocomposite foams; a) PUR 3, b) PUR 3 + 2 % OMMT, c) PUR 3 + 3 % OMMT, d) PUR 3 + 5 % OMMT and e) PUR 3 + 7 % OMMT.

SEM micrographs. The surface morphologies of PUR composite foams samples were investigated via scanning electron microscopy (SEM). The samples PUR 3 + 2 % OMMT, PUR 3 + 3 % OMMT, PUR 3 + 5 % OMMT, PUR 3 + 7 % OMMT, PUR 3 + 10 % OMMT and PUR 4 + 2 % OMMT were selected to understand the effect of OMMT incorporation and the presence of diamino-1,2-propylene as catalyst. As shown in Figs. 7 and 8, each sample was observed at 300 \times and 600 \times .

The PUR 3 + 7 % OMMT, PUR 3 + 10 % OMMT and PUR 4 + 2 % OMMT formulations constituted organized, closed and regular sized cells. The shape of the alveolus was orbicular, with an estimated diameter of 100 $\mu\text{m} \times 100 \mu\text{m}$, 100 $\mu\text{m} \times 50 \mu\text{m}$ and 250 $\mu\text{m} \times 80 \mu\text{m}$, respectively. On the other hand, the PUR 3 + 2 % OMMT, PUR 3 + 3 % OMMT and PUR 3 + 5 % OMMT formulations constituted open cells with micro-alveolus. The size of these latter formulations were regular and their diameter was estimated to be 100 \times 100 μm for PUR 3 + 2 % OMMT foam, 60 $\mu\text{m} \times 60 \mu\text{m}$ for PUR 3 + 3 % OMMT foam and 50 $\mu\text{m} \times 40 \mu\text{m}$ for the PUR 3 + 5 % OMMT foams.

It could be concluded that the cell size decreases with increasing OMMT content in the foams. Starting from the 7 % OMMT sample, the cell structure becomes closed and thicker. The size of the cells confirms the change in density,

which increases with increasing added clay content. On the other hand, the influence of the diamino 1,2-propane catalyst was to give thick and closed cells after being opened for a foam load of 2 % OMMT.

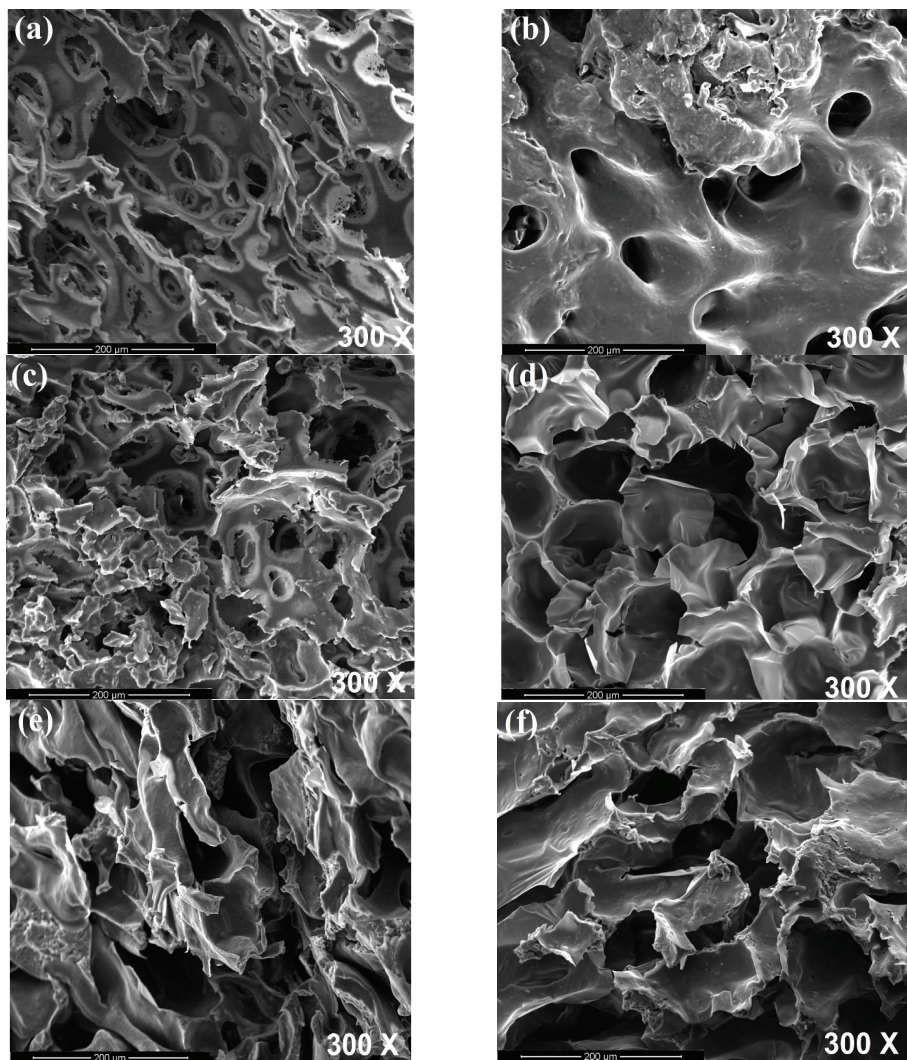


Fig. 7. SEM micrographs of nanocomposite foams at 300 \times magnification; a) PUR 3 + 2 % OMMT, b) PUR 3 + 3 % OMMT, c) PUR 3 + 5 % OMMT, d) PUR 3 + 7 % OMMT, e) PUR 3 + 10 % OMMT and f) PUR 4 + 2 % OMMT.

Jahanmardi *et al.*⁵¹ observed the same phenomenon, where a decrease in size and an increase in the number/area of the alveoli were explained by the barrier effect of the clay, which leads to the reduction in the nucleation energy.

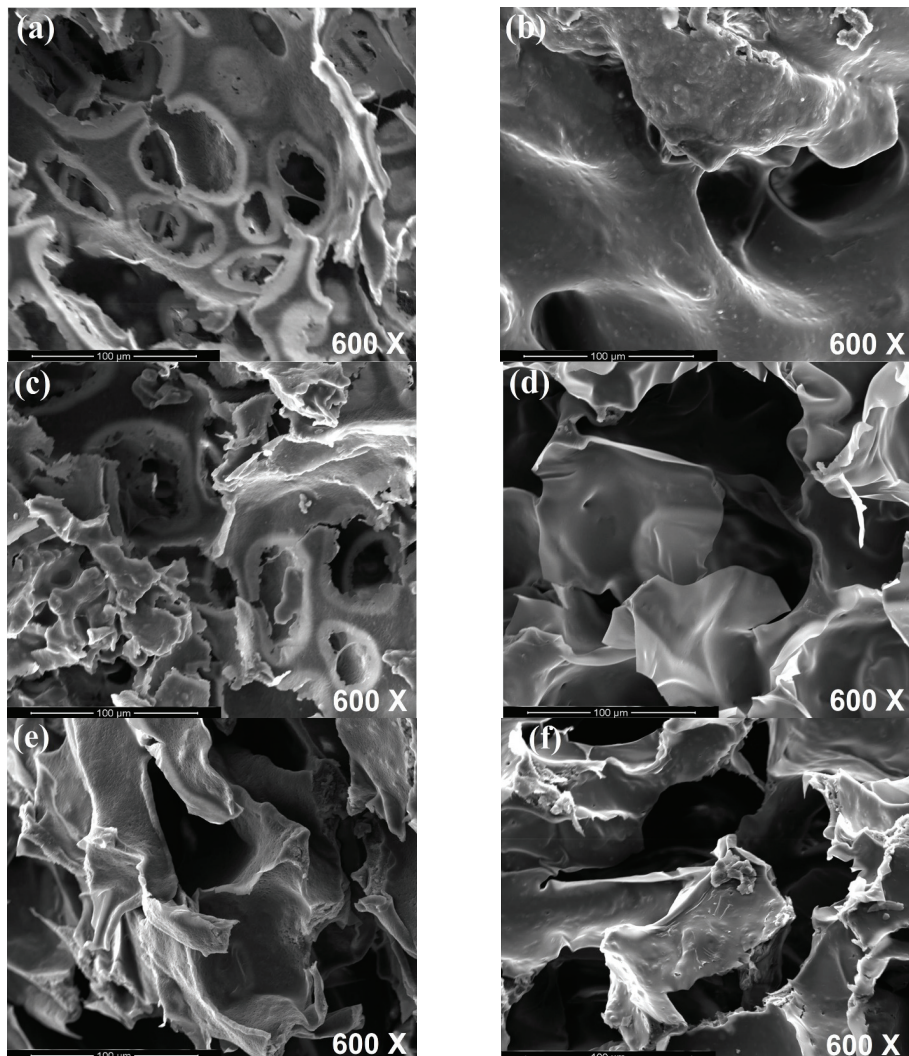


Fig. 8. SEM micrographs of nanocomposite foams; a) PUR 3 +2 % OMMT, b) PUR 3 + 3 % OMMT, c) PUR 3 + 5 % OMMT, d) PUR 3 + 7 % OMMT, e) PUR 3 + 10 % OMMT and f) PUR 4 + 2 % OMMT.

CONCLUSIONS

The purification and organophilic modification of the montmorillonite were successfully achieved. The distance between clay layers increased significantly after treatment. The PUR 4 sample, prepared using diamino-1,2-propane catalyst, shows the best mechanical properties, but it is not classified in the UL 94 V flammability test. The PUR/OMMT nanocomposites foam prepared using a twin-screw extruder in the counter-rotating mode assisted by the RIM process showed

interesting properties for the PUR 3 + 2 % OMMT composite. The retardant flame properties increased to 210 s for PUR 3 + 2 % OMMT and to 220 s for PUR 4 + 2 % OMMT, while PUR 3 was not classified according to the UL 94 HB flammability test.

SUPPLEMENTARY MATERIAL

Additional data are available electronically at the pages of journal website: <http://www.shd.org.rs/JSCS/>, or from the corresponding author on request.

ИЗВОД

ИЗРАДА ПОЛИУРЕТАНСКИХ ПЕНА/ОММТ НАНОКОМПОЗИТА ПОМОЋУ КОНТРА-РОТИРАЈУЋЕГ ДВОПУЖНОГ ЕКСТРУДЕРА

YASMINE MAHMOUD¹, ZITOUNI SAFIDINE¹ и HICHEM ZEGHIOUD²

¹Laboratoire de Chimie Macromoléculaire, Ecole militaire Polytechnique, BP 17, Bordj El Bahri, Algeria

²Laboratoire de Génie des Procédés, Université Badji Mokhtar, Annaba, Algeria

У овом раду је приказан нови поступак израде нанокомпозита на бази полиуретанске пене/органо-модификованих монтморилонита (PUR/OMMT), *in situ* полимеризацијом. За израду полиуретанских нанокомпозита коришћен је поступак реакционог бризгања (RIM – reaction injection moulding) у контра-ротирајућем двопужном екструдеру. Смеше полиола и кополимерног полиола (SRR) су интеркалиране између ОММТ слојева умешавањем у двопужном екструдеру. Састав PUR као и растојање између слојева у монтморилониту (MMT) су оптимизовани. Такође је анализиран утицај неких параметара као што су ОММТ садржај и врста катализатора (триетилендиамин за PUR 3 и триетилендиамин + диамино-1,2 пропан за PUR 4). Синтетисани материјали (OMMT, PUR и PUR/OMMT) су охарактерисани различitim методама: инфрацрвена спектроскопија са Фуријевим трансформацијама (FTIR), Рентгенска дифракција (XRD) и електронска скенирајућа микроскопија (SEM). Резултати запаљивости и огледа истезања за PUR 3 + OMMT пене су показали да оптимална својства поседује PUR 3 + 2 % OMMT узорак. PUR 4 пена је показала боља механичка својства и смањену запаљивост у односу на PUR 3 пену ($r = -\text{NCO} / -\text{OH} = 1,15$). Међутим, PUR 4 + 2 % OMMT композит је имао највише одложену дифузију пламена и изражену чврстоћу.

(Примљено 21. марта, ревидирано 14. септембра, прихваћено 18. септембра 2018)

REFERENCES

1. X. Cao, L. J. Lee, T. Widya, C. Macosko, *Polymer* **46** (2005) 775
2. L. Madaleno, R. Pyrz, A. Crosky, L.-R. Jensen, J. C. M. Rauhe, V. Dolomanova, A. M. M. V. de B. Timmons, J. J. C. Pinto, J. Norman, *Composites* **44** (2013) 1
3. S. Estravís, J. Tirado-Mediavilla, M. Santiago-Calvo, J. L. Ruiz-Herrero, F. Villafaña, M. Á. Rodríguez-Pérez, *Eur. Polym. J.* **80** (2016) 1
4. G. Sung, J. W. Kim, J. H. Kim, *J. Ind. Eng. Chem.* **44** (2016) 99
5. P. S. Khobragade, D. P. Hansora, J. B. Naik, A. Chatterjee, *Polym. Degrad. Stab.* **130** (2016) 194
6. Y. Gui, X. Liu, Y. Tian, N. Ding, Z. Wang, *Colloids Surfaces, A* **414** (2012) 274
7. L. Zhang, M. Zhang, Y. Zhou, L. Hu, *Polym. Degrad. Stab.* **98** (2013) 2784
8. X. Zheng, G. Wang, W. Xu, *Polym. Degrad. Stab.* **101** (2014) 32
9. N. Gama, L. C. Costa, V. Amaral, A. Ferreira, A. B. Timmons, *Compos. Sci. Technol.* **138** (2017)
10. L. Zhang, M. Zhang, Y. Zhou, L. Hu, *Polym. Degrad. Stab.* **98** (2013) 2784

11. W. Xi, L. Qian, Y. Chen, J. Wang, X. Liu, *Polym. Degrad. Stab.* **122** (2015) 36
12. W. Xi, L. Qian, Z. Huang, Y. Cao, L. Li, *Polym. Degrad. Stab.* **130** (2016) 97
13. R. Sonnier, B. Otazaghine, A. Viretto, G. Apolinario, P. Ienny, *Eur. Polym. J.* **68** (2015) 313
14. F. Salaün, M. Lewandowski, I. Vroman, G. Bedek, S. Bourbigot, *Polym. Degrad. Stab.* **96** (2011) 131
15. L. Gao, G. Zheng, Y. Zhou, L. Hu, G. Feng, M. Zhang, *Polym. Degrad. Stab.* **101** (2014) 92
16. A. Lorenzetti, S. Besco, D. Hrelja, M. Roso, E. Gallo, B. Schartel, M. Modesti, *Polym. Degrad. Stab.* **98** (2013) 2366
17. H.-B. Chen, Y.-Z. Wang, M. S. Soto, D. A. Schiraldi, *Polymer* **53** (2012) 5825
18. W. Xu, G. Wang, X. Zheng, *Polym. Degrad. Stab.* **111** (2015)
19. C. E. Corcionea, P. Prinari, D. Cannoletta, G. Mensitieri, A. Maffezzoli, *Int. J. Adhes. Adhes.* **28** (2008) 91
20. J. Pavličević, M. Špirkova, A. Strachota, K. M. Szecsenyić, N. Lazić, J. B. Simendić, *Thermochim. Acta* **509** (2010) 73
21. F. Cao, S. C. Jana, *Polymer* **48** (2007) 3790
22. Ł. Piszczyk, M. Strankowski, M. Danowska, J. T. Haponiuk, M. Gazda, *Eur. Polym. J.* **48** (2012) 1726
23. J. Xiong, Z. Zheng, H. Jiang, S. Ye, X. Wang, *Composites* **38** (2007) 132
24. N. Sarier, E. Onder, *Thermochim. Acta* **510** (2010) 113
25. B. Yıldız, M. O. Seydibeyoglu, F. S. Guner, *Polym. Degrad. Stab.* **94** (2009) 1072
26. M. Sonnenschein, B. L. Wendt, A. K. Schrock, J.-M. Sonney, A. J. Ryan, *Polymer* **49** (2008) 934
27. W. Wang, Y. Pan, H. Pan, W. Yang, K. M. Liew, L. Song, Y. Hu, *Compo. Sci. Technol.* **123** (2016) 212
28. J.-C. Yang, Z.-J. Cao, Y.-Z. Wang, D. A. Schiraldi, *Polymer* **66** (2015) 86
29. Y. Qian, W. Liu, Y. T. Park, C. I. Lindsay, R. Camargo, C. W. Macosko, A. Stein, *Polymer* **53** (2012) 5060
30. L. Song, Y. Hu, Y. Tang, R. Zhang, Z. Chen, W. Fan, *Polym. Degrad. Stab.* **87** (2005) 111
31. N. Pauzi, R. A. Majid, M. H. Dzulkifli, M. Y. Yahya, *Composites* **67** (2014) 521
32. G. Verma, A. Kaushika, A. K. Ghosh, *Prog. Org. Coat.* **99** (2016) 282
33. J. Xiong, Y. Liu, X. Yang, X. Wang, *Polym. Degrad. Stab.* **86** (2004) 549
34. F. J. Lejj, J. H. Dane, in *Analytical and numerical solutions of the transport equation for an exchangeable solute in a layered soil*, Lowell T. Frobish, Ed., Auburn university, Alabama, 1989 (<https://aurora.auburn.edu/bitstream/handle/11200/1542/0696-AGRO.pdf?sequence=1&isAllowed=y>)
35. S. Lv, W. Zhou, S. Li, W. Shi, *Eur. Polym. J.* **44** (2008) 1613
36. J. M. Yeh, C. T. Yao, C. F. Hsieh, L. H. Lin, P. L. Chen, J. C. Wu, H. C. Yang, C. P. Wu, *Eur. Polym. J.* **44** (2008) 3046
37. H. Moustafa, H. Galliard, L. Vidal, A. Dufresne, *Eur. Polym. J.* **87** (2017) 188
38. M. El Achaby, H. Ennajih, F. Z. Arrakhiz, A. El Kadib, R. Bouhfid, E. Essassi, A. Qais, *Composites* **51** (2013) 310
39. Ö. Eğri, K. Salimi, S. Eğri, E. Pişkin, Z. M. O. Rzayev, *Carbohydr. Polym.* **137** (2016) 111
40. L. Biesekia, F. Bertella, H. Treichel, F. G. Penha, S. B. C. Pergher, *Mat. Res.* **16** (2013) 1122

41. D. E. Kherroub, M. Belbachir, S. Lamouri, L. Bouhadjar, K. Chikh, *Orient. J. Chem.* **29** (2013) 1429
42. C. S. Carriço, T. Fraga, V. M. D. Pasa, *Eur. Polym. J.* **85** (2016) 53
43. A. Hejna , M. Kirpluks, P. Kosmela, U. Cabulisb, J. Haponiuk, Ł. Piszczyk, *Ind. Crop Prod.* **95** (2017) 113
44. H. Zeghioud, S. Lamouri, Y. Mahmoud, T. Hadj-Ali, *J. Serb. Chem. Soc.* **80** (2015) 1435
45. M. C. Saha, M. E. Kabir, S. Jeelani, *Mat. Sci. Eng., A - Struct.* **479** (2008) 213
46. E. A. Moawed, M. A. El-Hagrasy, N. E. M. Embaby, *J. Taiwan Inst. Chem. Eng.* **70** (2017) 382
47. W. Yang, S. Luo, B. Zhang, Z. Huang, X. Tang, *Appl. Surf. Sci.* **254** (2008) 7427
48. H. Lian, W. Chang, Q. Liang, C. Hu, R. Wang, L. Zu, Y. Liu, *RSC Adv.* **7** (2017) 46221
49. H. Liu, J. Gao, W. Huang, K. Dai, G. Zheng, C. Liu, C. Shen, X. Yan, J. Guo, Z. Guo, *Nanoscale* **8** (2016) 12977
50. M. Kumar, J. S. Chung, B.-S. Kong, E. J. Kim, S. H. Hur, *Mater. Lett.* **106** (2013) 319
R. Jahanmardi, B. Kangarloo, A. R. Dibazar, *J. Nanostructure Chem.* **1** (2013) 1.